JACS
JOURNAL OF THE AMERICAN CHEMICAL SOCIETY

Article

pubs.acs.org/JACS

α-Cationic Arsines: Synthesis, Structure, Reactivity, and Applications

Jonathan W. Dube,[†,‡] Yiying Zheng,[‡] Walter Thiel,[‡] and Manuel Alcarazo*[,†]

[†]Institut für Organische und Biomolekulare Chemie, Georg-August-Universität Göttingen, Tammannstraße 2, 37077 Göttingen, Germany

[‡]Max-Planck-Institut für Kohlenforschung, Kaiser-Wilhelm-Platz 1, 45470 Mülheim an der Ruhr, Germany

Supporting Information

ABSTRACT: A series of structurally differentiated cationic arsines containing imidazolium, cyclopropenium, formamidinium, and pyridinium substituents have been synthesized through short and scalable routes. Evaluation of the donor properties of these compounds by IR spectroscopy and DFT calculations reveals similar σ-electron-releasing abilities for all of them; however, their π-acceptor properties are strongly influenced by the nature of the positively charged group. We describe the coordination chemistry of the newly prepared α-cationic arsines toward different metal centers and their reactivity in the presence of strong oxidants to afford cationic As(V) species. Their unique electronic properties have been exploited in Pt(II) catalysis to develop a new catalyst with remarkable activity in the cycloisomerization of enynes to trisubstituted cyclopropanes. To the best of our knowledge, this is the first report on the use of α-cationic arsine ligands in catalysis.

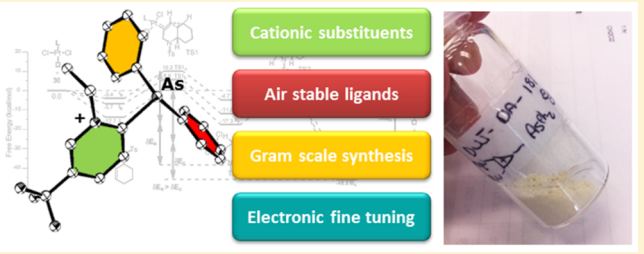

INTRODUCTION

Although the differences in steric parameters between phosphines and arsines of identical substitution pattern are minor and basically derived from the longer As−C bond, their electronic properties are fundamentally distinct. The increased s-character of the lone pair in arsines results in a less directional and lower-energy HOMO that accounts for the poorer σ-donor properties of these ligands. In addition, the π-acceptor character in arsines is also diminished compared to that of structurally related phosphines because of the more diffuse nature of the σ*(As−C) orbitals compared to that of σ*(P−C) ones, and the gradual reduction of electronegativity when moving down to the heavier elements of a group.[1] These unique electronic attributes account for the numerous applications that arsines have found as ancillary ligands in organic transformations such as cycloisomerizations,[2] carbonylations,[3] hydroacylations,[4] (de)hydrogenations,[5] or the cross-coupling of organostannanes with organic electrophiles, also known as the Stille reaction.[6]

During the past few years, our group has been interested in the design and synthesis of strong acceptor ligands and the study of their influence on catalytic processes where high Lewis acidity at the metal is beneficial at the rate-determining step of the cycle. In this regard, our strategy has been based on the formal replacement of a neutral −R substituent on phosphines by a positively charged organic group.[7] The charge thus introduced considerably reduces the donor capacity of the resulting cationic ligand and confers acceptor properties that often overtake those of classical acceptor ligands such as phosphites or polyfluorinated phosphines.[8] Taking advantage of these new attributes, a series of Au(I) and Pt(II) catalysts depicting enhanced activities for the hydroarylation of alkynes have been recently developed.[9]

Driven by this research program, we envisaged that modification of the intrinsic electronic properties of arsines by attachment of positively charged groups might result in an interesting new family of ligands with potential utility in catalysis.[10] In the following we summarize our investigations on the synthesis and structure of several α-cationic arsines, evaluate the influence of the positive charge on their donor properties by experimental and theoretical methods, and demonstrate for the first time their practical application in catalysis.[11]

RESULTS AND DISCUSSION

Synthesis and Structure of Cationic Arsines. At the outset of our study, we attempted the preparation of imidazolium-substituted arsine **2** by reaction of IMes with the readily available Ph_2AsI (**1**)[12] following a protocol analogous to the one described for the synthesis of phosphine-stabilized arsenium cations.[13] Interestingly, although **2** is the only species observed by NMR analysis, an equilibrium between this adduct and the starting materials is proposed because addition of 1 equiv of TMSTfO to solutions of **2** quantitatively regenerates **1** together with an equimolar amount of the TMS-trapped carbene **4** (Scheme 1). Irrespective of the associative or dissociative nature of this equilibrium, its mere existence reflects the lability of the $C_{carbene}$−As bond when compared

Received: April 9, 2016
Published: May 23, 2016

DOI: 10.1021/jacs.6b03500
J. Am. Chem. Soc. 2016, 138, 6869−6877

Scheme 1. Synthesis of Imidazolium Substituted Arsines[a]

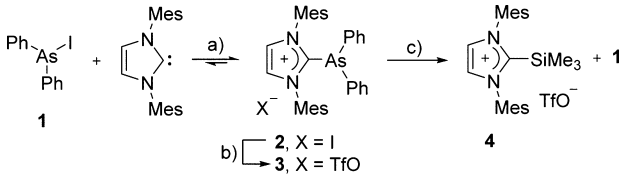

[a]Reagents and conditions (yields): (a) toluene (94%); (b) AgTfO, THF (94%); (c) TMSTfO, CH_2Cl_2 (93%).

with that of the nondative As−C_{Ph} bond (See the Supporting Information). In situ anion exchange in **2** from iodide to triflate employing AgTfO as alternative iodide trapping reagent suppresses this equilibrium and thus imparts heightened stability to the resulting compound **3**.

Crystals suitable for X-ray analysis were grown by slow diffusion of Et_2O into a saturated solution of **3** in dichloromethane, thus allowing the unambiguous confirmation of its connectivity (Figure 1). Particularly prominent in this structure

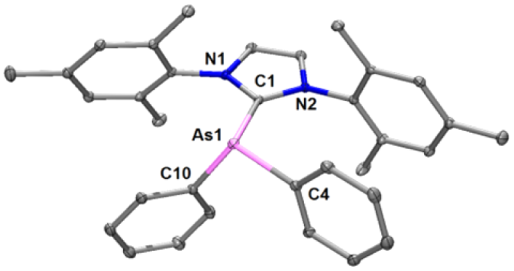

Figure 1. Molecular structure of **3** in the solid state. Hydrogen atoms and triflate anions are omitted for clarity. Anisotropic displacement parameter shown at 50% probability level.[14]

is the C1−As1 distance 1.9858(8) Å that is slightly longer than the other two C−As distances (C4−As1, 1.9468(9) Å and C10−As1, 1.9461(9) Å) probably due to the steric hindrance exerted by the two mesitylene substituents; the acute angles around As are a consequence of the decreased tendency to hybridization for the heavier pnictogen atoms (C1−As1−C10, 96.31(3)°; C10−As1−C4, 103.14(4)°; and C1−As1−C4, 101.81(3)°). These parameters define the geometry around the As atom as a distorted pyramid and are consistent with a lone pair of electrons on the arsenic center.

Preparation of analogue adducts **6** and **9**, both of them formally derived from very sensitive or simply unavailable carbene moieties, required a different synthesis route. In these cases 1-chloro cyclopropenium or 1-chloro formamidinium salts were treated with $Ph_2AsSiMe_3$ (**5**) in THF, affording the desired cationic arsines **6** and **9**, respectively, albeit in only moderate yields (Scheme 2a).[15−17] Further optimization of the reaction conditions revealed a drastic improvement in the yield of **6** when 1-iodocyclopropenium salts were employed instead of their chloro-substituted analogues. Because the formation of Me_3SiI as byproduct is thermodynamically less favorable than that of Me_3SiCl, it can only be the better leaving group properties of the iodide anion that account for this result. These optimized conditions were also applied to the synthesis of 1- and 4-substituted pyridinium arsines **10** and **11** from 1-methyl-4-iodo- and 1-methyl-2-iodopyridinium triflates, respectively.

Finally, cationic arsine **13**, decorated with an electron-withdrawing $-CF_3$ moiety on the pyridinium ring, could only

Scheme 2. General Synthesis of Cationic Arsines[a]

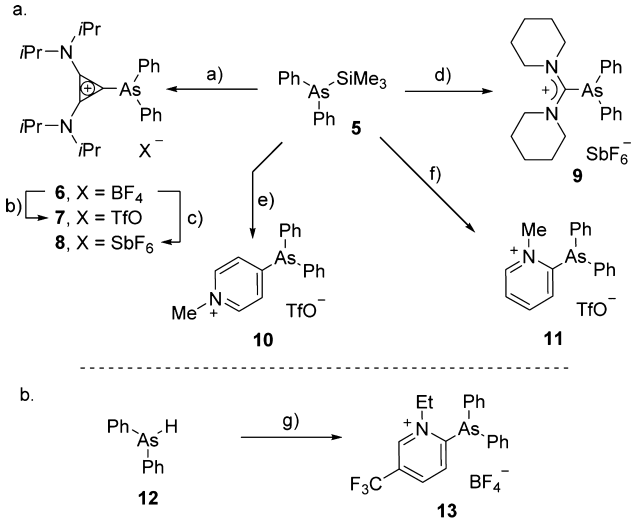

[a]Reagents and conditions (yields): (a) Path a, 1-iodo-2,3-bis-(diisopropylamino) cyclopropenium tetrafluoroborate, THF, 60 °C, (83%); path b, KTfO, acetonitrile, (90%); path c, $NaSbF_6$, acetonitrile, (88%); path d, 1-chloro-1,1-di(piperidin) formamidinium hexafluoroantimonate, THF, 65 °C, (62%); path e, 1-methyl-4-iodo-pyridinium triflate, CH_2Cl_2, rt, (47%); path f, 1-methyl-2-iodo-pyridinium triflate, CH_2Cl_2, rt, (38%). (b) Path g, 1-ethyl-4-trifluoromethyl-2-chloropyridinium tetrafluoroborate, THF, reflux, (19%).

be prepared by condensation of the corresponding 2-chloro pyridinium salt with diphenylarsine **12** in refluxing THF. Even under these conditions, its yield was rather low. Once isolated, compounds **6**, **11**, and **13** are remarkably stable to air and moisture in the solid state and could be stored for months at room temperature without evident decomposition. In contrast, handling of **9** and **10** requires the employment of Schlenck techniques.

Figure 2 depicts the molecular structure diagrams of **7** and **13** in the solid state (See the Supporting Information for the X-ray structures of **11**). Their metrics are very similar to those found in **3**. It is worth highlighting the slightly shorter C1−As1 bond distance in **7** (1.937(3) Å) compared with that in **3** (1.9858(8) Å) or **13** (1.9865(13) Å); this is surely a consequence of the smaller steric demand exerted by the cyclopropenium architecture.

Electronic Properties of Cationic Arsines. At this point, the donor endowment of the newly prepared arsines was evaluated by analysis of the CO stretching frequencies in *trans*-[RhCl(CO)L_2] complexes **14**−**18** (Scheme 3). Comparison of the IR spectra reveals within experimental error that the di(piperidin)-formamidinium substituent is able to impart acceptor properties on the final arsine stronger than those on pyridinium or cyclopropenium groups. However, the effect of pyridinium moieties is amenable to stereoelectronic modification by simple introduction of substituents in their skeleton. Hence, arsine **13** (bearing a very electron withdrawing $-CF_3$ group attached to the pyridinium ring) behaves as the weakest donor along the complete series.

Although the IR frequencies already allow the relative classification of cationic arsines by their donor properties, the determination of their Tolman electronic parameter (TEP) would be even more informative, specifically for comparison with other ligands. The TEP values can be reliably estimated from DFT computations, thereby eliminating the necessity of

DOI: 10.1021/jacs.6b03500
J. Am. Chem. Soc. 2016, 138, 6869−6877

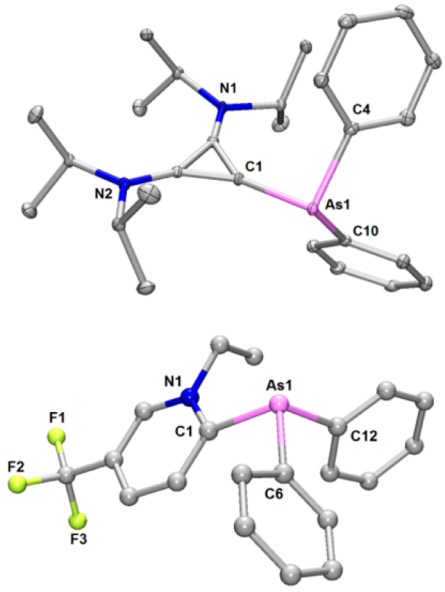

Figure 2. Molecular structures of **7** (top) and **13** (bottom) in the solid state. Hydrogen atoms and triflate anions are omitted for clarity. Anisotropic displacement parameter is shown at 50% probability level.[14]

Scheme 3. Carbonyl Stretching Frequencies in RhCl(CO)(arsine)$_2$ Complexes[a]

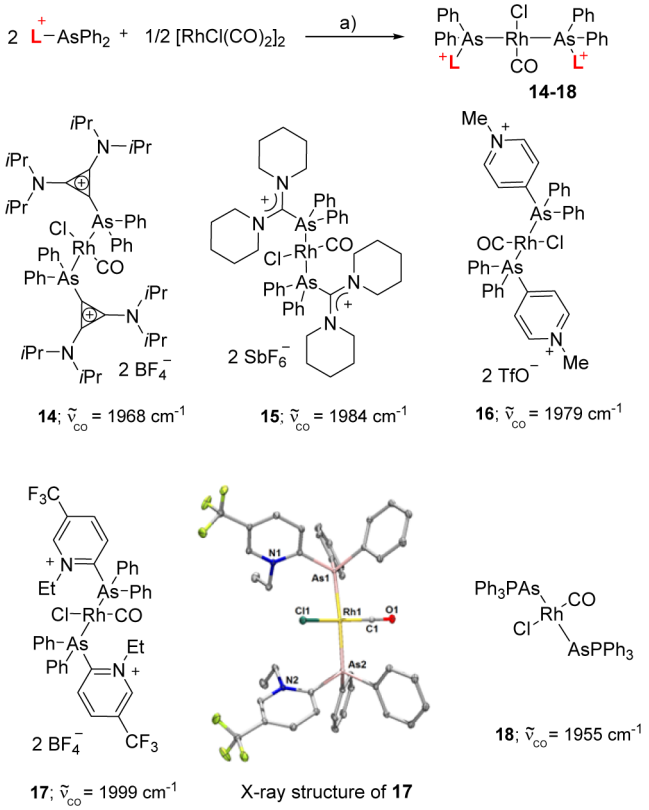

[a]Reagents and conditions (yields): (a) THF, rt; **14** (87%); **15** (90%); **16** (94%); **17** (93%); **18**(96%). IR spectra were recorded from solid samples of the title compounds.

handling $Ni(CO)_4$. Hence, using the Gaussian 09 suite of programs,[18] a series of 13 typical $LNi(CO)_3$ complexes (L = arsines and phosphines) were optimized without any symmetry constraints using the B3LYP-D3 functional, the LanL2DZ effective core potential for Ni, and the def2-TZVP basis set for all other atoms (see the Supporting Information).[19] Each local minimum was verified by an analytical frequency calculation.

The predicted harmonic stretching frequencies (A_1 ν_{co}) define the computed electronic parameter (CEP) for each ligand. According to the method described by Clot,[20] these CEP values were plotted against the experimental TEPs, and a regression analysis was performed (R^2 = 0.986) to establish the relation between these quantities: TEP = 1.0168 CEP − 105.0 cm^{-1} (Figure 3). This equation allows the prediction of the

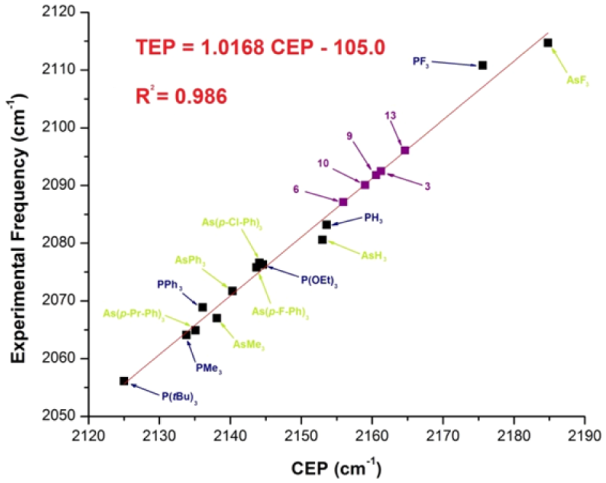

Figure 3. Correlation between CEP and TEP (both in cm^{-1}) and calculated TEPs for **3**, **6**, **9**, **10**, and **13**.

TEPs for cationic arsines **3**, **6**, **9**, **10**, and **13**, which range between 2087 and 2097 cm^{-1} (Table 1). These parameters

Table 1. Predicted TEPs and θ for Cationic Arsines

entry	ligand	TEP	θ (deg)
1	**3**	2092.6	178
2	**6**	2087.4	154
3	**9**	2092.2	156
4	**10**	2091.3	150
5	**13**	2097.0	144

confirm the trend previously observed on the Rh scale, implying that cationic arsines possess electron-donating ability poorer than that of any typical arsine or phosphite. Only PF_3 or AsF_3 surpass them in this realm. Finally, the Tolman cone angles θ of these ligands were determined from the optimized geometries of the $LNi(CO)_3$ complexes.

In an attempt to gain deeper insight into the electronic structure of these new arsines and their interaction with metals, a natural bond orbital (NBO) analysis was carried out at the B3LYP-D3/def2-TZVP level using NBO version 3.1. The optimized gas-phase structures of all $[L–AsPh_2]^+$ derivatives (see the Supporting Information) are consistent with the geometries observed experimentally in the solid state. Interestingly, inspection of the frontier orbitals in $AsPh_3$, **3**, **6**, **9**, **10**, and **13** reveals that the HOMOs of all these compounds have substantial lone pair character at As. The HOMO is much lower in energy in the cationic arsines than in Ph_3As (−6.16 eV), indicating that the magnitude of the σ-donation is reduced in all new arsines compared with Ph_3As. It is also noteworthy

DOI: 10.1021/jacs.6b03500
J. Am. Chem. Soc. 2016, 138, 6869–6877

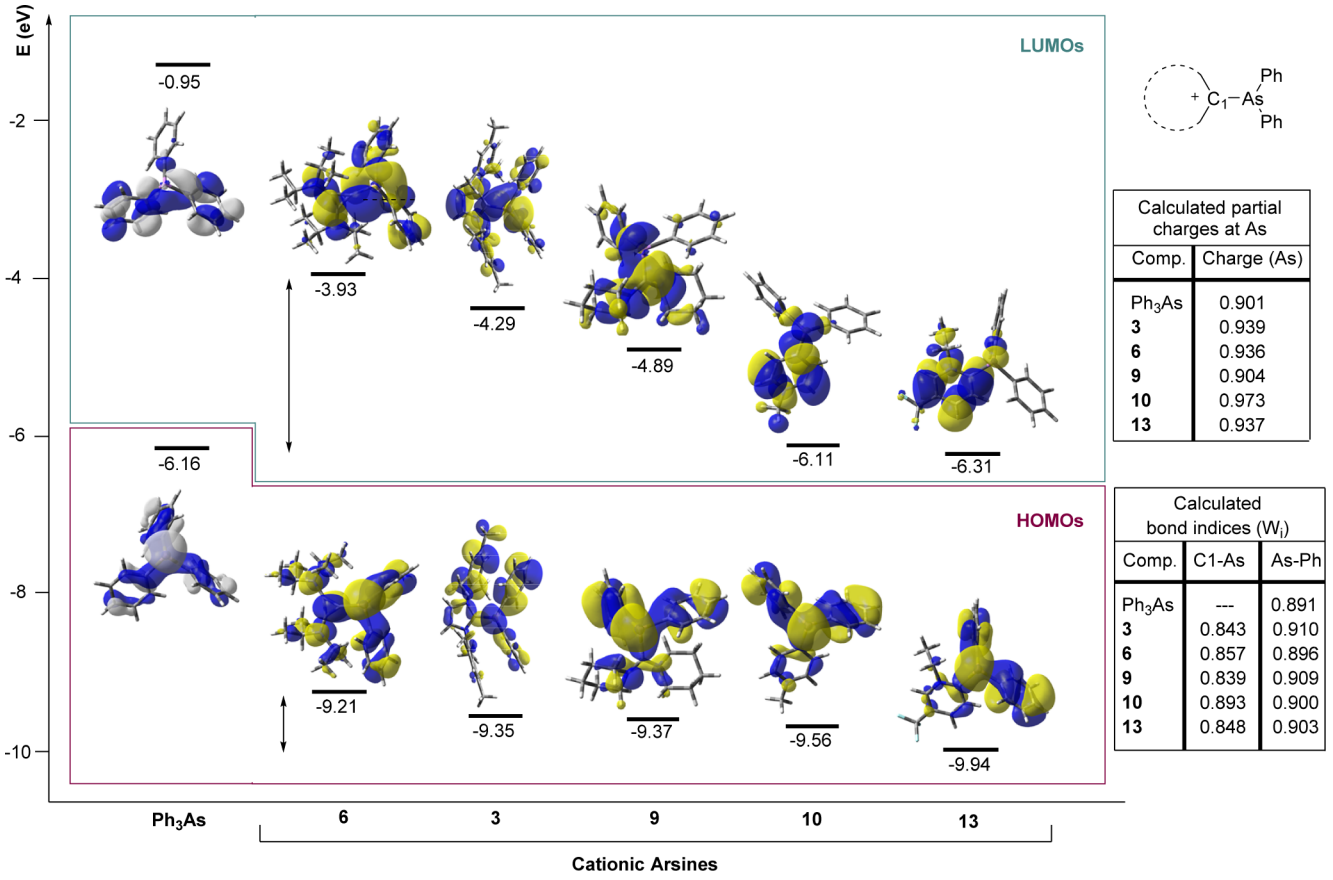

Figure 4. Frontier orbitals for arsines **3**, **6**, **9**, **10**, and **13** calculated at the B3LYP-D3/def2-TZVP level.

that the HOMOs of **3**, **6**, **9**, **10**, and **13** lie in a relatively tight range of energies, between −9.21 eV (HOMO of **6**) and −9.94 eV (HOMO of **13**). Hence, the σ-donor ability of all cationic arsines is only little influenced by the nature of the positively charged substituent attached to the central As (Figure 4). The NBO partial charges calculated for the central pnictogen in the gas-phase cations are also very similar, which indirectly supports this assessment.

In sharp contrast, the nature of the cationic substituent strongly influences the energies and shapes of the LUMOs. This is reflected in the different contributions from the π-systems of the cationic moieties to this orbital. As shown in Figure 4, the LUMOs have progressively lower energies and get gradually more localized on the −onium group in the sequence from cyclopropenium to imidazolium, formamidinium, and pyridinium. This suggests that the systematic reduction in the donor properties of ligands **6**, **3**, **9**, **10**, and **13** can be attributed primarily to an enhanced π-acceptor ability in the arsines that bear cationic groups able to accumulate electron density in their π-system.

Coordination and Oxidation Studies. Cationic arsines represent rare examples of ligands; no metal complex derivatives have been reported to date. The isolation of Rh derivatives **14**−**17** encouraged us to do a deeper study of their reactivity toward different metal fragments. Specifically, driven by our program aimed at elucidating ligand effects on π-acid catalysis, we targeted the synthesis of Au(I) and Pt(II) complexes. To our delight, all tested ligands reacted satisfactorily with $(Me_2S)AuCl$, or K_2PtCl_4 to afford the corresponding complexes **19**−**26** in excellent yields (Scheme 4); the connectivities were unambiguously confirmed by X-ray diffraction analysis (Figure 5 for **20** and **25**; see the Supporting Information for the structure of **26**).

Detailed analysis of the crystal structures reveals two trends upon coordination: a slight shortening of all As−C bonds that can be attributed to the higher electrophilic character of As after coordination and a significant increase of all C−As−C angles that overrides the steric effect caused by the incoming metal fragment. Taking **20** as example, each of the three angles (C1−As1−C10, 106.74(9)°; C10−As1−C4, 104.05(10)°; and C1−As1−C4, 103.91(9)°) is on average 5° wider than in the free ligand. This points to a hybridization closer to sp^3 at the As center after coordination, in order to maximize the orbital overlap with the metal.

The successful preparation of Au(I) derivatives, which benefits from the presence of a low-lying σ^*(As−C1) orbital in cationic arsines, prompted us to attempt the isolation of metal complexes derived from other d^{10} species. Hence, we treated **6** with an equimolar amount of $Pd(PPh_3)_4$. This caused the precipitation of a new yellow salt, the cationic part of which contained two Pd atoms, as evidenced by its ESI-MS spectrum. Moreover, ^{31}P NMR spectroscopy indicated the presence of PPh_3 still coordinated to the Pd centers. After extensive experimentation, we managed to grow single crystals of **27** that were suitable for X-ray analysis; the atom connectivity is shown in Figure 6. It is postulated that upon coordination, massive back-donation from Pd(0) to the σ^*(As−C1) orbital promotes the oxidative insertion of Pd into this bond and the generation of a Pd(II) arsenide that subsequently dimerizes. Flanking cyclopropenylidene and PPh_3 ligands complete the coordina-

DOI: 10.1021/jacs.6b03500
J. Am. Chem. Soc. 2016, 138, 6869−6877

Scheme 4. Synthesis of Au and Pt Complexes[a]

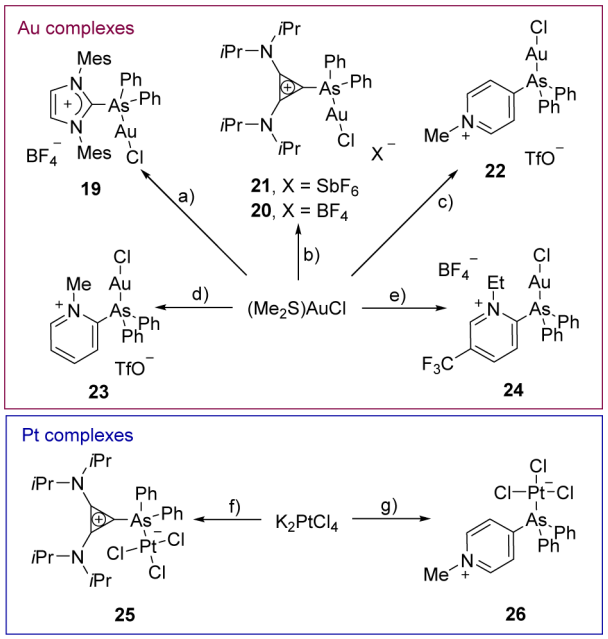

[a]Reagents and conditions (yields): (a) **3**, CH_2Cl_2, rt, (92%); (b) **6**, CH_2Cl_2, −20 °C, (89%) or **8**, CH_2Cl_2, −20 °C., (92%); (c) **10**, CH_2Cl_2, −20 °C, (92%); (d) **11**, CH_2Cl_2,, −20 °C, (95%); (e) **13**, CH_2Cl_2, −20 °C, (96%); (f) **6**, CH_3CN, rt, (95%); (g) **10**, CH_3CN, rt, (n.d.).

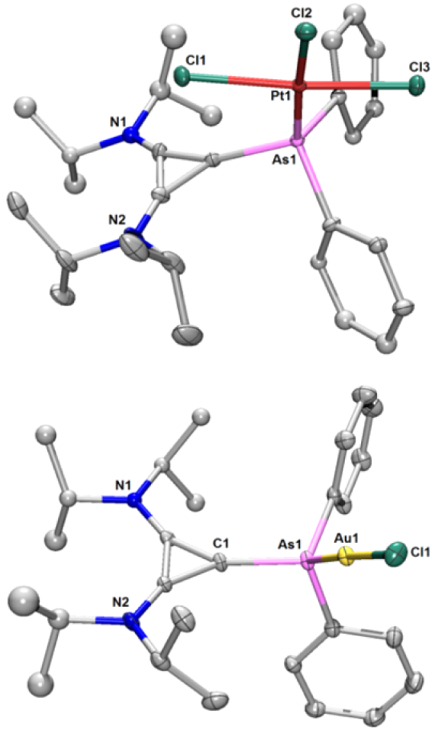

Figure 5. Molecular structures of **25** (top) and **21** (bottom) in the solid state. Hydrogen atoms and anions are omitted for clarity. Anisotropic displacement parameter is shown at 50% probability level.[14]

tion sphere of each Pd atom.[21] The isolation of this unexpected species upon reaction with an extremely electron-rich metal

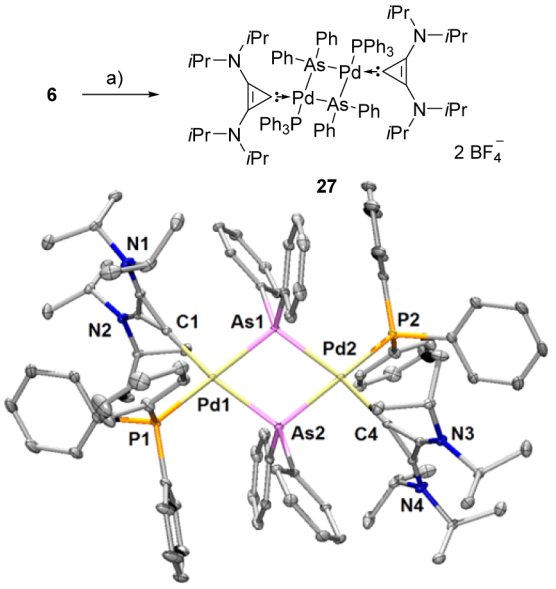

Figure 6. Synthesis and molecular structure of **27** in the solid state. Reagents and conditions (yields): (a) $Pd(PPh_3)_4$, toluene, 100 °C (53%). Hydrogen atoms and anions are omitted for clarity. Anisotropic displacement parameter is shown at 50% probability level.[14]

species shows the application limits of cationic arsines as ancillary ligands.

Finally, we proceeded to explore whether the nonshared electron pairs in cationic arsines could react with strong oxidants to afford the corresponding As(V) species. Taking **6** as model, its oxidation with XeF_2 in dichloromethane was attempted resulting in the quantitative formation of a new species **28** that gave rise to a new ^{19}F NMR signal at $\delta = -77.8$ ppm (Scheme 5). The connectivity of this compound was also

Scheme 5. Reactivity of Cyclopropenium Arsines towards Oxidants[a]

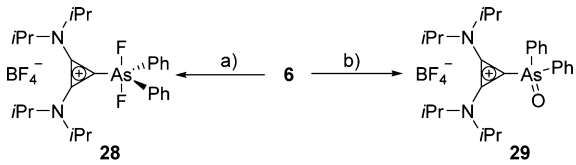

[a]Reagents and conditions (yields): (a) XeF_2, CH_2Cl_2, rt, (98%); (b) *m*-CPBA, CH_2Cl_2, rt, (85%).

confirmed by X-ray crystallography: it corresponds to the desired cationic As(V) difluoride. Both fluoride anions occupy the axial positions of the trigonal bipyramidal environment around the As (As1−F1, (1.8114(9) Å; As1−F2, (1.8103(9) Å), whereas the phenyl and cyclopropenium groups stay at the equatorial plane. Compound **28** constitutes the only known example of an As(V) complex containing a cyclopropenylidene carbene ligand (Figure 7).[22] Oxidation with *m*-CPBA proceeds cleanly and affords the corresponding arsine oxide **29**.

CATALYSIS

Having obtained an overview of the general reactivity of cationic arsines, we decided to evaluate the suitability of these ligands in catalysis. As a preliminary study, we compared the performance of the newly prepared ligands with that of $AsPh_3$,

DOI: 10.1021/jacs.6b03500
J. Am. Chem. Soc. 2016, 138, 6869−6877

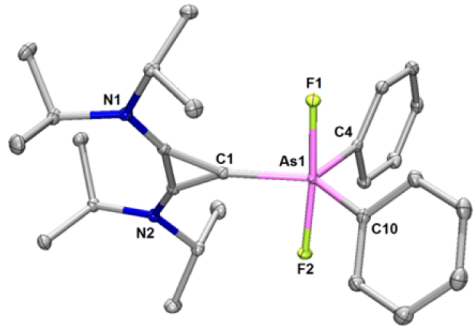

Figure 7. Molecular structure of **28** in the solid state. Hydrogen atoms and anions are omitted for clarity. Anisotropic displacement parameter is shown at 50% probability level.[14]

PPh_3, and $P(OPh)_3$ in the Pt-catalyzed cycloisomerization of enyne **30** to trisubstituted cyclopropane **31**.[23] This specific benchmark reaction was chosen for two main reasons. When $PtCl_2$ is used as catalyst similar substrates cyclize cleanly but very slowly even at high temperatures, whereas employment of significantly stronger π-acidic catalysts, such as those based on Au(I), invariably leads to lower yields and the formation of undesired polymers when the alkyne moiety is terminal, as in **30**.[24] In fact, the best catalyst described for this specific substrate is $GaCl_3$, and even in that case only 12% yield of the product was isolated.[24c] Finally, during initial experiments, we already noticed the superior efficacy of $AsPh_3$ in this process when compared with that of PPh_3 or $P(OPh)_3$. Taken together, this cyclization seems ideal to test the ability of our newly prepared cationic arsines for fine-tuning the electronic properties of Pt(II) centers.

We were delighted to see that the catalytic activity of the species formed by activation of **25** with $AgSbF_6$ clearly surpasses that of any other catalyst tested; the relative initial rate constants k_{rel} of the reaction promoted by **25** versus that of $PtCl_2$ or $Ph_3As/PtCl_2$ mixtures are 153.5 and 7.7, respectively, under otherwise identical conditions (Figure 8).[25] Under these conditions, compound **31** could be isolated in 75% yield. On the other hand, the use of complex **26** bearing a stronger π-acceptor pyridinium derivative did not have the expected

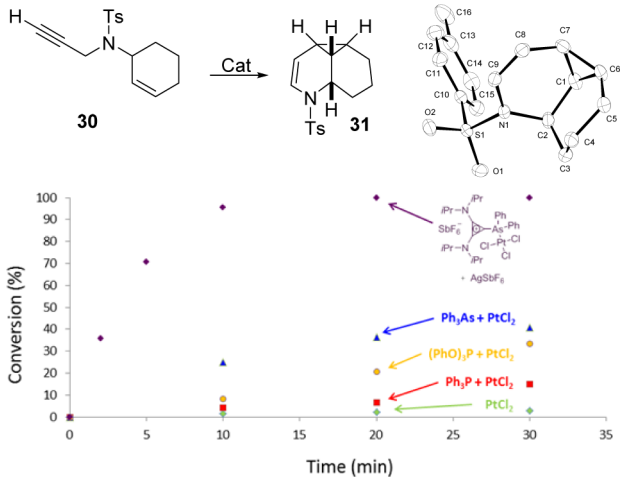

Figure 8. Ligand effect on the Pt-catalyzed cycloisomerization of **30** to cyclopropane **31**. Reagent and conditions: (a) **30** (0.05 M), Pt precatalyst, 2 mol %, $AgSbF_6$ 2 mol %, DCE, 80 °C. Conversions determined by gas chromatography.

beneficial effect on the cycloisomerization process; a series of experiments consistently afforded low yields of product and evidence of both polymer formation and catalyst decomposition. This striking behavior perfectly compares with the results described for Au-based catalysts and probably defines a scenario where the Lewis acidity of Pt has been excessively increased.[24c]

DFT Calculations on the Reaction Mechanism. To gain more detailed insight, the reaction mechanism was explored through density functional theory (DFT). Geometries were optimized using the B3LYP-D3 functional combined with the def2-SVP effective core potential and basis set for Pt and with the def2-SVP basis set for all other atoms.[26] The same level of theory was employed for frequency calculations to confirm each stationary point to be either a minimum or transition state (TS) structure. Single-point calculations with the larger def2-TZVP basis[27] at the gas-phase optimized geometries were carried out with inclusion of continuum solvation[28] (see the Supporting Information for further details).

Free energy profiles (ΔG at 298 K, see Supporting Information for numerical results) were computed for the cyclization of **30** to **31** using PPh_3, $AsPh_3$ and a simplified version of **8** (with Me_2N substituents instead of i-Pr_2N substituents) as ancillary ligands. They are displayed in Figure 9. The calculated free energies of coordination of **30** to the three catalysts are −3.8, −5.7, and −12.7 kcal/mol, respectively, indicating exergonic formation of the intermediate complexes $\mathbf{I}_{a\text{-}c}$. The trend in the computed thermodynamic stabilities can be traced back to the frontier orbitals of the catalysts (Figure 10). The lowest unoccupied molecular orbital (LUMO) has a very similar shape in all three catalysts (σ*P/As−Pt), but its energy clearly decreases in the following order: Ph_3P-$PtCl_2$ > Ph_3As-$PtCl_2$ > **8**-$PtCl_2$. Because a low LUMO energy correlates with a strong π-acidity of the catalyst, it is not surprising that the coordination of the alkyne to Pt is especially favorable when stronger acceptor ligands are employed.

The next step along the reaction coordinate involves the nucleophilic attack of the olefin at the activated alkyne forming the cyclopropyl intermediates $\mathbf{II}_{a\text{-}c}$ via transition states $\mathbf{TS1}_{a\text{-}c}$, respectively. Our calculations indicate that regardless of the ancillary ligand used these are the highest-energy transition states that govern the kinetics of the cycle. The beneficial effect of ligand **8** is clear because $\mathbf{TS1}_c$ lies 9.9 and 6.6 kcal/mol below $\mathbf{TS1}_a$ and $\mathbf{TS1}_b$, respectively. A comparison of the C−C distances in transition states $\mathbf{TS1}_{a\text{-}c}$ helps us to understand the stabilizing effect of **8** (Figure 11). The calculated C1−C3 and C1−C4 distances respectively are 1.96 and 2.39 Å in $\mathbf{TS1}_a$, 1.98 and 2.39 Å in $\mathbf{TS1}_b$, and much longer (2.15 and 2.45 Å) in $\mathbf{TS1}_c$, reflecting an earlier and thus energetically lower transition state in the reaction promoted by **8**.

The Pt carbenes $\mathbf{II}_{a\text{-}c}$ evolve via 1,2-H shifts to form the corresponding olefins coordinated to Pt, $\mathbf{III}_{a\text{-}c}$. These compounds are 34−39 kcal/mol more stable than their precursors $\mathbf{II}_{a\text{-}c}$, and the energies of the transition state leading to the product **31** are much lower than those of $\mathbf{TS2}_{a\text{-}c}$. Hence, the formation of **31** seems to be irreversible. Interestingly, $\mathbf{III}_c$ is the most stable intermediate in this series, making the release of the final product especially difficult when **8**-$PtCl_2$ is used as catalyst. However, in the framework of the energetic span model,[29] this catalyst is still the one that minimizes the energetic span (δE) for the complete catalytic cycle; therefore, it is the best one to accelerate the reaction under study.

DOI: 10.1021/jacs.6b03500
J. Am. Chem. Soc. 2016, 138, 6869−6877

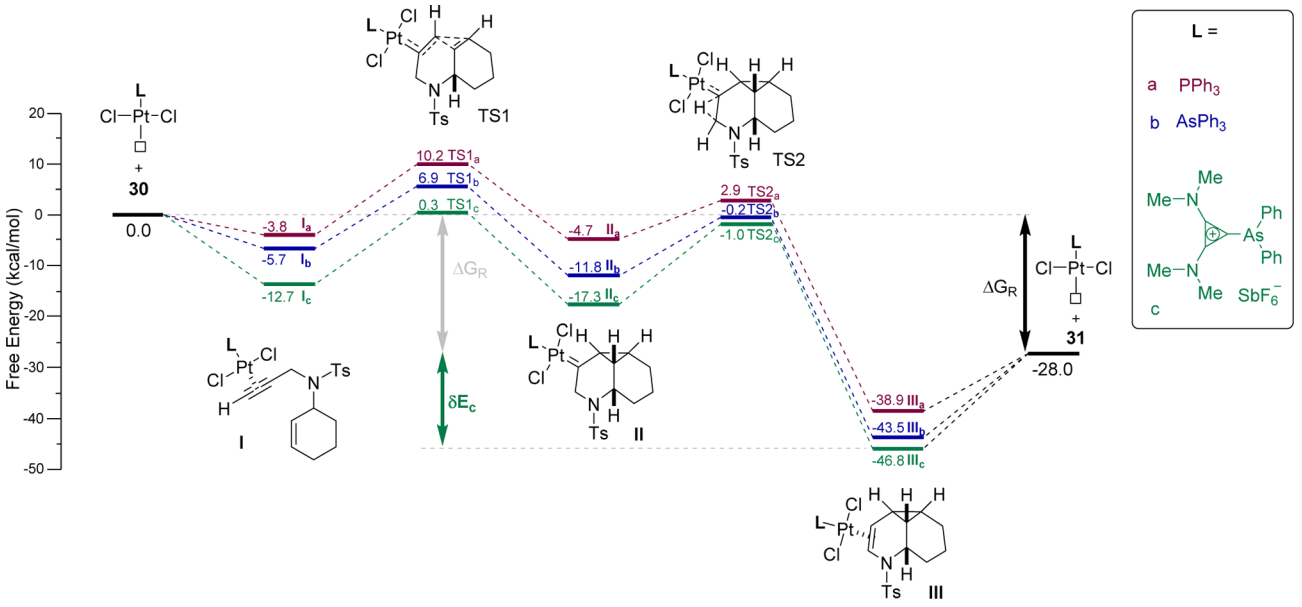

Figure 9. Free energy profiles (kcal/mol) for the cyclization of **30** into **31** in CH_2Cl_2.

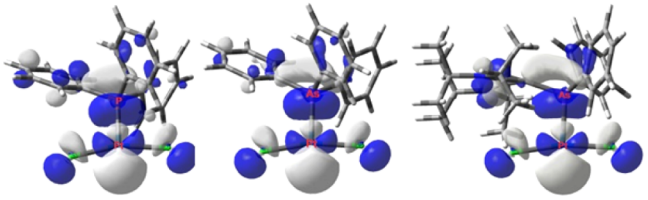

Figure 10. From left to right: LUMO of Ph_3P-$PtCl_2$ (E = −2.97 eV), Ph_3As-$PtCl_2$ (E = −3.06 eV), and **8**-$PtCl_2$ (E = −5.99 eV).

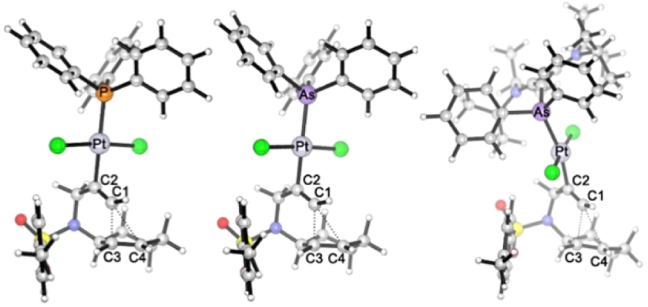

Figure 11. Optimized geometries of $\mathbf{TS1}_a$ (left): C1−C3, 1.96 Å; C1−C4, 2.39 Å; $\mathbf{TS1}_b$ (middle): C1−C3, 1.98 Å; C1−C4, 2.39 Å; $\mathbf{TS1}_c$ (right): C1−C3, 2.15 Å; C1−C4, 2.45 Å.

CONCLUSIONS

We describe herein the synthesis, electronic properties, and structural characterization of α-cationic arsines in which the positive charge is delocalized over heterocyclic systems of different nature. In contrast to already reported base-stabilized arsonium salts, α-cationic arsines can serve as ligands for a range of metal fragments, depicting donor abilities considerably weaker than those of their neutral counterparts. Exploiting this effect, we have developed a Pt catalyst with remarkable activity in the cycloisomerization of enynes to cyclopropanes. Studies toward further applications of these new ligands in other contexts and toward the development of their chiral versions are currently underway in our research group.

ASSOCIATED CONTENT

Supporting Information

The Supporting Information is available free of charge on the ACS Publications website at DOI: 10.1021/jacs.6b03500.

Crystallographic information file for compound **3**. (CIF)
Crystallographic information file for compound **6**. (CIF)
Crystallographic information file for compound **7**. (CIF)
Crystallographic information file for compound **11**. (CIF)
Crystallographic information file for compound **13**. (CIF)
Crystallographic information file for compound **14**. (CIF)
Crystallographic information file for compound **17**. (CIF)
Crystallographic information file for compound **20**. (CIF)
Crystallographic information file for compound **25**. (CIF)
Crystallographic information file for compound **26**. (CIF)
Crystallographic information file for compound **27**. (CIF)
Crystallographic information file for compound **28**. (CIF)
Crystallographic information file for compound **31**. (CIF)
Experimental procedures including the characterization data for all new compounds, additional crystallographic information, NMR spectra, and computational procedures including detailed numerical results and orbital plots. (PDF)

AUTHOR INFORMATION

Corresponding Author

*malcara@gwdg.de

Notes

The authors declare no competing financial interest.

DOI: 10.1021/jacs.6b03500
J. Am. Chem. Soc. 2016, 138, 6869−6877

■ ACKNOWLEDGMENTS

Financial support from the Fonds der Chemischen Industrie (Dozentenstipendium to M.A.) and European Commission (ERC Starting Grant to M.A.) is gratefully acknowledged. We also thank Prof. C. W. Lehmann, H. Tinnermann, and J. Rust for solving the X-ray structures and S. Holle for the initial preparation of **6**. J.W.D. is grateful to the Natural Sciences and Engineering Research Council of Canada (NSERC) for a postdoctoral fellowship.

■ REFERENCES

(1) Levanson, W.; Reid, G. In *Comprehensive Coordination Chemistry II*; McCleverty, J. A.; Meyer, T. J., Ed.; Pergamon: Oxford, 2003; pp 337−389.
(2) Trost, B. M.; Edstrom, E. D.; Carter-Petillo, M. B. *J. Org. Chem.* **1989**, *54*, 4489−4490.
(3) van der Veen, L. A.; Keeven, P. K.; Kamer, P. C. J.; van Leeuwen, P. W. N. M. *Chem. Commun.* **2000**, 333−334.
(4) Hong, Y. T.; Barchuk, A.; Krische, M. J. *Angew. Chem., Int. Ed.* **2006**, *45*, 6885−6888.
(5) (a) Tanabe, Y.; Kuriyama, S.; Arashiba, K.; Nakajima, K.; Nishibayashi, Y. *Organometallics* **2014**, *33*, 5295−5300. (b) Brayton, D. F.; Beaumont, P. R.; Fukushima, E. Y.; Sartain, H. T.; Morales-Morales, D.; Jensen, C. M. *Organometallics* **2014**, *33*, 5198−5202. (c) Allen, D. G.; Wild, S. B.; Wood, D. L. *Organometallics* **1986**, *5*, 1009−1015.
(6) (a) Ronson, T. O.; Carney, J. R.; Whitwood, A. C.; Taylor, R. J. K.; Fairlamb, I. J. S. *Chem. Commun.* **2015**, *51*, 3466−3469. (b) Bedford, R. B.; Betham, M.; Bruce, D. W.; Danopoulos, A. A.; Frost, R. M.; Hird, M. *J. Org. Chem.* **2006**, *71*, 1104−1110. (c) Baber, R. A.; Collard, S.; Hooper, M.; Orpen, A. G.; Pringle, P. G.; Wilkinson, M. J.; Wingad, R. L. *Dalton Trans.* **2005**, 1491−1498. (d) Amatore, C.; Bahsoun, A. A.; Jutand, A.; Meyer, G.; Ndedi Ntepe, A.; Ricard, L. *J. Am. Chem. Soc.* **2003**, *125*, 4212−4222. (e) Johnson, C. R.; Braun, M. P. *J. Am. Chem. Soc.* **1993**, *115*, 11014−11015. (f) Farina, V.; Krishnan, B. *J. Am. Chem. Soc.* **1991**, *113*, 9585−9595.
(7) (a) Alcarazo, M. *Chem. - Eur. J.* **2014**, *20*, 7868−7877. (b) Gaillard, S.; Renaud, J. L. *Dalton Trans.* **2013**, *42*, 7255−7270. (c) Canac, Y.; Maaliki, C.; Abdellah, I.; Chauvin, R. *New J. Chem.* **2012**, *36*, 17−27.
(8) (a) Kozma, Á.; Rust, J.; Alcarazo, M. *Chem. - Eur. J.* **2015**, *21*, 10829−10834. (b) Canac, Y.; Bijani, C.; Duhayon, C.; Chauvin, R. *Organometallics* **2013**, *32*, 4054−4057. (c) Vabre, B.; Canac, Y.; Duhayon, C.; Chauvin, R.; Zargarian, D. *Chem. Commun.* **2012**, *48*, 10446−10448. (d) Digard, E.; Andrieu, J.; Cattey, H. *Inorg. Chem. Commun.* **2012**, *25*, 39−42. (e) Abdellah, I.; Lepetit, C.; Canac, Y.; Duhayon, C.; Chauvin, R. *Chem. - Eur. J.* **2010**, *16*, 13095−13108. (f) Saleh, S.; Fayad, E.; Azouri, M.; Hierso, J. C.; Andrieu, J.; Picquet, M. *Adv. Synth. Catal.* **2009**, *351*, 1621−1628. (g) Canac, Y.; Debono, N.; Vendier, L.; Chauvin, R. *Inorg. Chem.* **2009**, *48*, 5562−5568. (h) Debono, N.; Canac, Y.; Duhayon, C.; Chauvin, R. *Eur. J. Inorg. Chem.* **2008**, *2008*, 2991−2999. (i) Andrieu, J.; Azouri, M.; Richard, P. *Inorg. Chem. Commun.* **2008**, *11*, 1401−1404. (j) Azouri, M.; Andrieu, J.; Picquet, M.; Richard, P.; Hanquet, B.; Tkatchenko, I. *Eur. J. Inorg. Chem.* **2007**, *2007*, 4877−4883.
(9) (a) Tinnermann, H.; Wille, C.; Alcarazo, M. *Angew. Chem., Int. Ed.* **2014**, *53*, 8732−8736. (b) Kozma, Á.; Deden, T.; Carreras, J.; Wille, C.; Petuškova, J.; Rust, J.; Alcarazo, M. *Chem. - Eur. J.* **2014**, *20*, 2208−2214. (c) Carreras, J.; Gopakumar, G.; Gu, L.; Gimeno, A. M.; Linowski, P.; Petuškova, J.; Thiel, W.; Alcarazo, M. *J. Am. Chem. Soc.* **2013**, *135*, 18815−18823. (d) Carreras, J.; Patil, M.; Thiel, W.; Alcarazo, M. *J. Am. Chem. Soc.* **2012**, *134*, 16753−16758. (e) Petuškova, J.; Bruns, H.; Alcarazo, M. *Angew. Chem., Int. Ed.* **2011**, *50*, 3799−3802.
(10) For the synthesis of pyridine-stabilized cationic arsines, see Braddock, J. M. F.; Coates, G. E. *J. Chem. Soc.* **1961**, *83*, 3208−3211.
(11) For a recent synthesis of a cationic dicloroarsonium cation, see Henne, F. D.; Dickschat, A. T.; Hennersdorf, F.; Feldmann, K.-O.; Weigand, J. J. *Inorg. Chem.* **2015**, *54*, 6849−6861.
(12) (a) Blicke, F. F.; Smith, F. D. *J. Am. Chem. Soc.* **1929**, *51*, 1558−1565. (b) Cullen, W. R.; Trotter, J. *Can. J. Chem.* **1961**, *39*, 2602−2603. A detailed experimental procedure and complete characterization of this compound can be found in the Supporting Information.
(13) For phosphine-stabilized arsenium salts, see (a) Kilah, N. L.; Wild, S. B. *Organometallics* **2012**, *31*, 2658−2666. (b) Weir, M. L.; Cade, I. A.; Kilah, N. L.; Zhou, X.; Wild, S. B. *Inorg. Chem.* **2009**, *48*, 7482−7490. (c) Kilah, N. L.; Petrie, S.; Stranger, R.; Wielandt, J. W.; Willis, A. C.; Wild, S. B. *Organometallics* **2007**, *26*, 6106−6113. (d) Burford, N.; Ragogna, P. J.; Sharp, K.; McDonald, R.; Ferguson, M. J. *Inorg. Chem.* **2005**, *44*, 9453−9460. (e) Porter, K. A.; Willis, A. C.; Zank, J.; Wild, S. B. *Inorg. Chem.* **2002**, *41*, 6380−6386. (f) Braddock, J. M. F.; Coates, G. E. *J. Chem. Soc.* **1961**, 3208−3211.
(14) CCDC 1408070−1408073, 1408075−1408077, 1408079, 1408081, 1408121, and 1472098−1472101 contain the crystallographic data for this paper. These data can be obtained free of charge from The Cambridge Crystallographic Data Centre via www.ccdc.cam.ac.uk/data_request/cif.
(15) This strategy has been quite successfully applied in our group for the synthesis of (poly)cationic phosphines, but to the best of our knowledge, it had no precedents in the case of arsines. See refs 9a and 9d and Haldón, E.; Kozma, Á.; Tinnermann, H.; Gu, L.; Goddard, R.; Alcarazo, M. *Dalton Trans.* **2016**, *45*, 1872−1876.
(16) Fenske, D.; Teichert, H.; Prokscha, H.; Renz, W.; Becher, H. J. *Monatsh. Chem.* **1980**, *111*, 177−191.
(17) (a) Weiss, R.; Engel, S. *Synthesis* **1991**, *1991*, 1077−1079. (b) Bouhadir, G.; Reed, R. W.; Reau, R.; Bertrand, G. *Heteroat. Chem.* **1995**, *6*, 371−375.
(18) Frisch, M. J.; Trucks, G. W.; Schlegel, H. B.; Scuseria, G. E.; Robb, M. A.; Cheeseman, J. R.; Scalmani, G.; Barone, V.; Mennucci, B.; Petersson, G. A.; Nakatsuji, H.; Caricato, M.; Li, X.; Hratchian, H. P.; Izmaylov, A. F.; Bloino, J.; Zheng, G.; Sonnenberg, J. L.; Hada, M.; Ehara, M.; Toyota, K.; Fukuda, R.; Hasegawa, J.; Ishida, M.; Nakajima, T.; Honda, Y.; Kitao, O.; Nakai, H.; Vreven, T.; Montgomery, J. A., Jr.; Peralta, J. E.; Ogliaro, F.; Bearpark, M.; Heyd, J. J.; Brothers, E.; Kudin, K. N.; Staroverov, V. N.; Kobayashi, R.; Normand, J.; Raghavachari, K.; Rendell, A.; Burant, J. C.; Iyengar, S. S.; Tomasi, J.; Cossi, M.; Rega, N.; Millam, J. M.; Klene, M.; Knox, J. E.; Cross, J. B.; Bakken, V.; Adamo, C.; Jaramillo, J.; Gomperts, R.; Stratmann, R. E.; Yazyev, O.; Austin, A. J.; Cammi, R.; Pomelli, C.; Ochterski, J. W.; Martin, R. L.; Morokuma, K.; Zakrzewski, V. G.; Voth, G. A.; Salvador, P.; Dannenberg, J. J.; Dapprich, S.; Daniels, A. D.; Farkas, O.; Foresman, J. B.; Ortiz, J. V.; Cioslowski, J.; Fox, D. J. *Gaussian 09*, revision D.01; Gaussian, Inc.: Wallingford, CT, 2009.
(19) (a) Becke, A. D. *J. Chem. Phys.* **1993**, *98*, 5648−5652. (b) Lee, C.; Yang, W.; Parr, R. G. *Phys. Rev. B: Condens. Matter Mater. Phys.* **1988**, *37*, 785−789. (c) Grimme, S.; Antony, J.; Ehrlich, S.; Krieg, H. *J. Chem. Phys.* **2010**, *132*, 154104.
(20) Perrin, L.; Clot, E.; Eisenstein, O.; Loch, J.; Crabtree, R. H. *Inorg. Chem.* **2001**, *40*, 5806−5811.
(21) For a related insertion into Se-C bonds, see Kozma, Á.; Petuškova, J.; Lehmann, C. W.; Alcarazo, M. *Chem. Commun.* **2013**, *49*, 4145−4147.
(22) For other As(V)-carbene complexes, see (a) Donath, M.; Bodensteiner, M.; Weigand, J. J. *Chem. - Eur. J.* **2014**, *20*, 17306−17310. (b) Arduengo, A. J., III; Davidson, F.; Krafczyk, R.; Marshall, W. J.; Schmutzler, R. *Monatsh. Chem.* **2000**, *131*, 251−265.
(23) For general reviews on π-acid catalysis, see (a) Dorel, R.; Echavarren, A. M. *Chem. Rev.* **2015**, *115*, 9028−9072. (b) Fürstner, A.; Davies, P. W. *Angew. Chem., Int. Ed.* **2007**, *46*, 3410−3449. (c) Hashmi, A. S. K.; Hutchings, G. J. *Angew. Chem., Int. Ed.* **2006**, *45*, 7896−7936.
(24) (a) Fürstner, A.; Szillat, H.; Stelzer, F. *J. Am. Chem. Soc.* **2000**, *122*, 6785−6787. (b) Fürstner, A.; Stelzer, F.; Szillat, H. *J. Am. Chem. Soc.* **2001**, *123*, 11863−11869. (c) Kim, S. M.; Lee, S. I.; Chung, Y. K. *Org. Lett.* **2006**, *8*, 5425−5427.

DOI: 10.1021/jacs.6b03500
J. Am. Chem. Soc. 2016, 138, 6869−6877

(25) The use of arsines as ancillary ligands in Au catalysis is scarce. For previous examples, see (a) Ramiro, Z.; Bartolomé, C.; Espinet, P. *Eur. J. Inorg. Chem.* **2014**, *2014*, 5499−5506. (b) Nieto-Oberhuber, C.; Muñoz, M. P.; López, S.; Jiménez-Núñez, E.; Nevado, C.; Herrero-Gómez, E.; Raducan, M.; Echavarren, A. M. *Chem. - Eur. J.* **2006**, *12*, 1677−1693.
(26) Weigend, F.; Ahlrichs, R. *Phys. Chem. Chem. Phys.* **2005**, *7*, 3297−3305.
(27) Weigend, F. *Phys. Chem. Chem. Phys.* **2006**, *8*, 1057−1065.
(28) (a) Foresman, J. B.; Keith, T. A.; Wiberg, K. B.; Snoonian, J.; Frisch, M. J. *J. Phys. Chem.* **1996**, *100*, 16098−16104. (b) Barone, V.; Cossi, M. *J. Phys. Chem. A* **1998**, *102*, 1995−2001. (c) Cossi, M.; Rega, N.; Scalmani, G.; Barone, V. *J. Comput. Chem.* **2003**, *24*, 669−681.
(29) Kozuch, S.; Shaik, S. *Acc. Chem. Res.* **2011**, *44*, 101−110.

DOI: 10.1021/jacs.6b03500
J. Am. Chem. Soc. 2016, 138, 6869−6877